



Fur -Dam regulatory interplay at an internal promoter of the enteroaggregative Escherichia coli Type VI secretion *scil* gene cluster

Yannick R Brunet, Christophe S Bernard, E. Cascales

► To cite this version:

Yannick R Brunet, Christophe S Bernard, E. Cascales. Fur -Dam regulatory interplay at an internal promoter of the enteroaggregative Escherichia coli Type VI secretion *scil* gene cluster. Journal of Bacteriology, 2020. hal-02534983

HAL Id: hal-02534983

<https://amu.hal.science/hal-02534983>

Submitted on 7 Apr 2020

HAL is a multi-disciplinary open access archive for the deposit and dissemination of scientific research documents, whether they are published or not. The documents may come from teaching and research institutions in France or abroad, or from public or private research centers.

L'archive ouverte pluridisciplinaire **HAL**, est destinée au dépôt et à la diffusion de documents scientifiques de niveau recherche, publiés ou non, émanant des établissements d'enseignement et de recherche français ou étrangers, des laboratoires publics ou privés.

**Fur – Dam Regulatory Interplay at An Internal Promoter
of the Enteroaggregative *Escherichia coli* Type VI Secretion *scil* Gene Cluster.**

Yannick R. Brunet[†], Christophe S. Bernard[¶], and Eric Cascales*

Running head: Regulation of the EAEC *scil* T6SS gene cluster.

Laboratoire d'Ingénierie des Systèmes Macromoléculaires (LISM), Institut de Microbiologie de la Méditerranée (IMM), CNRS – Aix-Marseille Université UMR7255, 31 chemin Joseph Aiguier, 13402 Marseille Cedex 20, France.

* To whom correspondence should be addressed. E-mail: cascales@imm.cnrs.fr

[†] Current address: Department of Microbiology and Immunobiology, Harvard Medical School, 77 Avenue Louis Pasteur, Boston, MA, 02115 USA.

[¶] Current address: Laboratoire de Chimie Bactérienne (LCB), Institut de Microbiologie de la Méditerranée (IMM), CNRS – Aix-Marseille Université UMR7283, 31 chemin Joseph Aiguier, 13402 Marseille Cedex 20, France.

Characters count (including spaces): 48,000

Tables: 0

Figures: 7

Supplemental material: 2 Figures

ABSTRACT

The type VI secretion system (T6SS) is a weapon widespread in Gram-negative bacteria that delivers effectors into target cells. The T6SS is a highly versatile machine as it can target both eukaryotic and prokaryotic cells, and it has been proposed that T6SS are adapted to the specific needs of each bacterium. The expression of T6SS gene clusters and the activation of the secretion apparatus are therefore tightly controlled. In enteroaggregative *Escherichia coli* (EAEC), the *sciI* T6SS gene cluster is subjected to a complex regulation involving both the ferric uptake regulator Fur and Dam-dependent DNA methylation. In this study, an additional, internal, promoter was identified within the *sciI* gene cluster using +1 transcriptional mapping. Further analyses demonstrated that this internal promoter is controlled by a mechanism strictly identical to that of the main promoter. The Fur binding box overlaps with the -10 transcriptional element and a Dam methylation site, GATC-32. Hence, the expression of the distal *sciI* genes is repressed and the GATC-32 site is protected from methylation in iron-rich conditions. The Fur-dependent protection of GATC-32 was confirmed by *in vitro* methylation assay. In addition, the methylation of GATC-32 negatively impacts Fur binding. The expression of the *sciI* internal promoter is therefore controlled by iron availability through Fur regulation whereas Dam-dependent methylation maintains a stable ON expression in iron-limited conditions.

IMPORTANCE

Bacteria use weapons to deliver effectors into target cells. One of these weapons, the type VI secretion system (T6SS), assembles a contractile tail acting as a spring to propel a toxin-loaded needle. Its expression and activation therefore need to be tightly regulated. Here we identified an internal promoter within the *sciI* T6SS gene cluster in enteroaggregative *E. coli*. We then show that this internal promoter is controlled by Fur and Dam-dependent methylation. We further demonstrate that Fur and Dam compete at the -10 transcriptional element to finely tune the expression of T6SS genes. We propose that this elegant regulatory mechanism allows the optimum production of the T6SS in conditions where enteroaggregative *E. coli* may encounter competing species.

65 INTRODUCTION

66 The fate of microbial communities is governed by communication, cooperation and
67 competition mechanisms between microorganisms (1-9). Bacteria therefore developed an
68 arsenal of signalling, sensing and antagonistic activities. To eliminate competitors, bacteria
69 evolved distinct mechanisms: release of antibiotics or bacteriocins in the extracellular
70 medium, as well as delivery of toxins directly into the target cell (10-12). One of the delivery
71 apparatuses, the type VI secretion system (T6SS), transports effectors into competing bacteria
72 using a mechanism similar to that used by contractile injection systems such as
73 bacteriophages and R-pyocins (13-19). This secretion apparatus is constituted of a ~ 600-nm
74 long cytoplasmic needle-like structure composed of an inner tube tipped by a spike complex
75 that is used to penetrate the membrane of the target cell (12, 14, 19). The inner tube is
76 wrapped by an outer sheath that is assembled under an extended metastable conformation (20,
77 21). The tail tube/sheath complex is built on a baseplate that is anchored to the cell envelope
78 by a membrane complex (22-29). Tail tube/sheath assembly, which can be visualised *in vivo*
79 by fluorescence microscopy, is completed in a few tens of seconds (30-32). Contraction of the
80 sheath powers the propulsion of the inner tube to deliver effectors into the target cell (15, 17,
81 31, 33-35). Effectors are usually charged within the inner tube lumen or loaded onto the spike
82 complex via direct interactions with the VgrG/PAAR spike or via adaptor proteins (36-45).

83 The T6SS is a very efficient mechanism and hence is an important player in the
84 regulation of the microbiota (7, 46). Bacteria equipped with this apparatus colonize more
85 efficiently the environmental niche and hence have a better access to the resources (47-51).
86 Most of the T6SS gene clusters are not constitutively expressed and T6SS-dependent
87 antagonistic activities are usually deployed once cells experience stress or nutrient starvation
88 conditions (52-57). T6SS gene clusters are therefore subjected to a tight regulation that

involves sensing of the environmental conditions (52, 53, 55). Most known regulatory mechanisms are hijacked by T6SSs for their regulation: transcriptional activators and repressors, alternate sigma factors, histone-like proteins, two-component transduction cascades, or quorum-sensing systems (52, 53). In addition, a number of T6SSs are post-translationally activated by a threonine phosphorylation pathway in response to cell damages or envelope stresses (58).

Enteroaggregative *Escherichia coli* (EAEC) is equipped with two functional T6SSs, named Sci1 (T6SS-1 subfamily) and Sci2 (T6SS-3 subfamily) (59, 60). These two T6SSs confer antagonistic activities but are not expressed in the same conditions, suggesting that T6SS-mediated anti-bacterial activities are required in two conditions that EAEC may encounter during its life cycle (31, 44). The *sci2* gene cluster is expressed during infection conditions and is activated in laboratory conditions when cells are grown in a synthetic medium mimicking the macrophage environment (59). This *sci2* gene cluster is under the control of the AraC-like AggR transcriptional regulator (59), which also modulates the expression of most biofilm determinants (59, 61), suggesting that the Sci2 T6SS is required for eliminating competing bacteria during aggregation, a phenomena that occurs during host colonization. By contrast, the *sci1* gene cluster is expressed in minimal synthetic media, and has been shown to be under the dual control of the ferric uptake repressor (Fur) and Dam-dependent methylation (62).

To gain further information on the *sci1* gene cluster organization, we defined its operon structure. RT-PCR experiments showed that all genes are contiguous suggesting that all the genes are present on a single mRNA or on several overlapping mRNAs. Using +1 transcriptional mapping, we confirmed the existence of a promoter region upstream the first gene of the cluster but revealed an additional promoter located upstream the *EC042_4532*

gene, within the *EC042_4531* gene coding sequence. We further identified a Fur-binding sequence overlapping with the -10 transcriptional box and demonstrated that Fur binds with high affinity and prevents RNA polymerase access to the promoter. Sequence analyses showed that this Fur box overlaps with a GATC Dam methylation site, GATC-32. *In vivo*, we showed that Fur prevents methylation of the GATC-32 site when cells grew in iron-replete conditions. *In vitro* competition experiments confirmed that Fur prevents GATC-32 methylation. In addition, we observed that Dam-dependent methylation of GATC-32 decreases the affinity of Fur for its Fur box. Taken together, our results demonstrate that a second functional, internal promoter controls the expression of T6SS *sciI* genes and that this promoter is under a regulatory mechanism identical to the main promoter.

RESULTS AND DISCUSSION

Operon structure of the *sciI* T6SS gene cluster. We previously reported that the promoter located upstream the *tssB* gene, *i.e.*, the first gene of the EAEC *sciI* T6SS gene cluster, contains operator sequences for the Ferric uptake regulator, Fur, as well as an overrepresentation of GATC motifs which are targets of the DNA adenine methylase Dam. Using *in vivo* and *in vitro* Fur binding and methylation assays, we delineated the contribution of these two regulators on the expression of the *tssB* gene (62). However, whether additional or internal promoters exist, and whether the entire gene cluster is subjected to this regulatory control remained undetermined. The EAEC *sciI* gene cluster is a ~ 26-kb DNA fragment present on the *pheU* pathogenicity island (Fig. 1A; 59). Prediction of the open reading frames (ORF) within this fragment shows that it encodes 21 gene products including the 14 T6SS core components, a toxin-immunity pair, and accessory genes or of unknown function (genes *tssB* to *tssE*, see Fig. 1A). With the exception of a large intergenic sequence (162-pb between

the *hcp* and the *clpV* genes), most of the start and stop codons of contiguous genes overlap or are separated by few (< 8) nucleotides (see Fig S1 in supplemental material). This genomic organization suggests that translational coupling must occur, and that the expression of these genes must be coordinated. To test whether the *sciI* gene cluster is organized as a single genetic unit, or constituted of several operons, we performed reverse-transcriptase - polymerase chain reactions (RT-PCR) using oligonucleotides designed for the amplification of each gene junction (numbered 1-21; see Fig. 1A). RT-PCR experiments were performed on purified total RNAs extracted from cells grown in *SciI*-inducing medium (SIM) (Fig. 1B; upper panel). As controls, RT-PCR reactions were performed on purified genome DNA (Fig. 1B, middle panel), as well as on the total RNA preparation but in absence of reverse transcriptase to test for DNA contamination (Fig. 1B, lower panel). As shown on Fig. 1B, RT-PCR products with expected sized were obtained for each gene junction of the *sciI* gene cluster from DNA or cDNA, but not from RNA (Fig. 1B, lanes 2-21), suggesting that the 21 genes are co-transcribed. As expected, the *Ec042_4523* ORF, upstream the first gene of the *sciI* cluster, and in the reverse orientation compared to the *tss* genes, is not co-transcribed with *tssB* (Fig. 1B, lane 1). These results suggest that all the *sciI* genes are present on a unique polycistronic mRNA, or that overlapping mRNAs are expressed from internal promoters.

An additional promoter is located upstream *EC042_4532*. To identify potential internal promoter(s), we used an *in silico* approach. Analysis of the T6SS *sciI* gene cluster using the BProm algorithm (Softberry; available at <http://linux1.softberry.com/berry.phtml>) suggested the existence of an additional promoter with a σ^{70} -10 element upstream the *EC042_4532* gene. To test whether an internal promoter is present upstream of *Ec042_4532*, we used 5'-RACE assay. mRNAs were extracted from EAEC cells grown in SIM and subjected to primer extension. The putative *tssB* promoter, was also included in this assay.

The results showed that transcription of the *tssB* mRNA starts at the base A, located 73 bases upstream the ATG start codon of *tssB* (colored red in Fig. 2A). The *tssB* transcription starts are therefore compatible with the putative -10 and -35 transcription boxes identified through *in silico* analyses in our previous study (62) (Fig. 2A). A transcriptional start was also detected upstream the *EC042_4532* gene, suggesting the existence of an active internal promoter. The position of the identified transcriptional start (base G located 117 bases upstream the ATG of *EC042_4532*, colored red in Fig. 2B) is compatible with the location of the -10 element predicted by the BProm algorithm (Fig. 2B).

***In silico* sequence analyses of the *EC042_4532* promoter region identify Fur and Dam sites overlapping with the -10 element.** Interestingly, the BProm computer program also identified a putative Fur binding box in the *EC042_4532* promoter region (hereafter called Fur-32). This putative operator sequence overlaps with the -10 of transcription (Fig. 2B and 2C). This situation is reminiscent of the main promoter, which is repressed by the Fur protein in an iron-dependent manner (62). One of the Fur boxes contained in the *tssB* promoter contains a Dam-dependent methylation site (Fig. 2A), and we previously reported that Fur and Dam compete at this specific site to fine tune the expression of the *sciI* gene cluster (62). Strikingly, a GATC motif is also found within the putative Fur-32 box of the *EC042_4532* promoter (Fig. 2C, hereafter called GATC-32). Taken together, the *in silico* sequence analyses raised the question whether the internal promoter is under a similar regulatory mechanism as the *tssB* main promoter.

The *P₄₅₃₂-lacZ* translational fusion is responsive to iron limitation and Fur. To test whether the expression of the internal promoter is regulated by Fur, we engineered a low copy plasmid-borne translational fusion of a 570-bp fragment comprising the *EC042_4532* promoter (from -450 to +120 relative to the transcriptional +1, called hereafter *P₄₅₃₂*) to *lacZ*.

The β -galactosidase activity of this P_{4532} -*lacZ* translational fusion was monitored in the EAEC *lacZ* strain or its *fur* isogenic mutant, in presence or absence of the iron chelator 2,2'-di-pyridyl (dip). Figure 3 shows that the expression of the P_{4532} translational fusion increased ~ 6-fold in the WT strain upon treatment with the iron chelator. Compared to the WT strain in absence of iron chelator, the activity of the translational fusion increased ~ 13-fold in the *fur* isogenic background. Treatment of the *fur* mutant strain with 2,2'-dipyridyl had no additional effect on the activity of the P_{4532} -*lacZ* translational reporter fusion (data not shown). From these activities, we concluded that the expression from the P_{4532} promoter is repressed by the Fur transcriptional regulator in an iron-dependent manner.

Fur binds to the P_{4532} promoter and limits access to the RNA polymerase. To test whether Fur binds the *EC042_4532* promoter region *in vitro*, the purified *E. coli* Fur protein and the radiolabeled P_{4532} 570-bp fragment were used for electrophoretic mobility shift assays (EMSA). As controls, and as previously published (62), Fur bound to the *sciI* promoter, yielding two bands due to the presence of two Fur boxes, but did not retard the Fur-independent *sci2* promoter (Fig. 4A, lanes 8-10). Fur also shifted the P_{4532} fragment in presence of iron, its co-repressor (Fig. 4A, lanes 1-5; Fig. 4B). This shift was strictly dependent on metal-bound Fur, as no band retardation could be observed when the fragment and the purified regulator were incubated in presence of the metal chelator EDTA (Fig. 4A, lane 6). By contrast, control experiments showed that the σ^{54} enhancer binding protein NtrC did not bind the P_{4532} fragment (Fig. 4A, lane 7). From these data, we conclude that Fur binds to the P_{4532} promoter *in vitro*, likely to the putative Fur-32 box.

Fur repression is usually caused by preventing access of the RNA polymerase (RNAP) to the promoter. We hypothesized that such a mechanism might be likely at promoter P_{4532} as the putative Fur-32 box overlaps with the -10 RNAP-binding element (Fig. 2B). We therefore

tested whether σ^{70} -RNAP holoenzyme binds to the P_{4532} promoter and whether Fur influences σ^{70} -RNAP binding. Fig. 4C shows that the σ^{70} -RNAP complex binds to the P_{4532} promoter (Fig. 4C, lanes 1-3) and that pre-incubation of the P_{4532} fragment with Fur prevents binding of the σ^{70} -RNAP, demonstrating that Fur and RNAP compete for binding on P_{4532} (Fig. 4C, lanes 4-6; Fig. 4D).

Dam methylation at the GATC-32 site decreases RNAP binding to the P_{4532} promoter. To gain insight on the contribution of Dam to the regulation of $EC042_4532$, we measured the β -galactosidase activity of the P_{4532} -*lacZ* translational fusion in *dam* and *fur-dam* EAEC strains. Deletion of *dam* did not cause a significant variation of the activity of the promoter fusion compared to its parental wild-type strain (Fig. 3). By contrast, the activity of the promoter fusion in the *fur-dam* strain increased ~ 16 -fold compared to the wild-type strain, and ~ 1.4 -fold compared to the *fur* mutant. These results show that Dam and Fur have additive negative effects on the regulation at the P_{4532} promoter, and that the contribution of Dam is masked in presence of Fur. Based on these results, we hypothesized that GATC-32 methylation affects RNAP binding. A Dam-methylated P_{4532} fragment was subjected to EMSA with the reconstituted σ^{70} -RNAP complex. As shown in Fig. 4C and Fig. 4D, σ^{70} -RNAP binding was diminished on the methylated P_{4532} fragment.

Fur-Dam competition at the P_{4532} promoter. The observation that the Dam effect was masked by Fur *in vivo* raised the idea that, similarly to the P_{sci1} situation, Fur binding to the Fur-32 box prevents Dam-methylation of the GATC-32 site. To test this hypothesis, *in vitro* and *in vivo* assays were conducted.

Fur binding at the P_{4532} promoter prevents GATC-32 methylation in vitro. To test the impact of Fur binding on GATC-32 methylation *in vitro*, we added purified Dam methylase to radiolabeled P_{4532} fragments pre-incubated or not with purified Fur protein. The P_{4532}

234 fragments were then used for enzymatic digestion using enzymes that cleave GATC motifs
235 (Fig S2 in supplemental material). We used the advantage that the GATC-32 site is part of a
236 larger palindromic sequence, TgatcA, which is the target for BclI, a restriction enzyme that is
237 sensitive to Dam methylation (Fig S2 in supplemental material). In addition to GATC-32, the
238 P_{4532} fragment contains a GATC site at position 149 (GATC¹⁴⁹) that does not overlap with a
239 Fur box (Fig S2 in supplemental material). Fig. 5A shows that, as expected, incubation with
240 the Dam methylase caused methylation of the GATC sites as P_{4532} is cleaved in three
241 fragments when incubated with DpnI, an enzyme that specifically recognizes methylated
242 GATC motifs. In agreement with this result, P_{4532} was resistant to MboI and BclI, two
243 enzymes that are sensitive to GATC adenine methylation (Fig. 5A, middle panel). When the
244 P_{4532} fragment was pre-incubated with Fur, only the GATC¹⁴⁹ site was digested by DpnI. By
245 contrast, only the GATC-32 site was digested by MboI or BclI (Fig. 5A, right panel). These
246 experiments demonstrate that in presence of Fur, GATC¹⁴⁹ is methylated whereas GATC-32
247 is not, suggesting that Fur protects GATC-32 methylation by steric occlusion.

248 *Fur binding at the P_{4532} promoter prevents GATC-32 methylation in vivo.* The methylation
249 status of the P_{4532} GATC sites was then tested *in vivo*. The pGE573 plasmid bearing the P_{4532} -
250 *lacZ* fusion was extracted from various genetic backgrounds, the *EcoR1-BamH1* fragment
251 comprising the P_{4532} promoter was purified and the methylation state of GATC-32 was
252 assessed by restriction. In the WT strain grown in LB medium, the MboI and BclI enzymes
253 cleaved GATC-32 (Fig. 5B, left panel), revealing that this site is un-methylated. The absence
254 of methylation is likely due to the presence of Fur bound to the Fur box overlapping with
255 GATC-32 as GATC-32 was methylated in the *fur* isogenic background (Fig. 5B, right panel)
256 or when WT cells were grown in presence of the 2,2'-dipyridyl iron chelator (Fig. 5B, third
257 panel from left).

Taken together, the results of the *in vitro* and *in vivo* Dam methylation assays demonstrate that Fur binding on the Fur-32 box prevents access of the Dam methylase to the GATC-32 site in iron rich conditions. By contrast, Fur repression is relieved in iron limiting conditions and the GATC-32 site is then methylated.

GATC-32 Dam methylation decreases the affinity of Fur to the P_{4532} promoter. The observation that the GATC-32 site is methylated once Fur repression is relieved raised the question whether methylation of the GATC-32 motif interferes with Fur binding. We therefore performed mobility shift assays with Fur using the P_{4532} fragment, methylated by Dam *in vitro*. Fig. 6 shows that methylation of GATC-32 caused a significant decrease of affinity of Fur for the P_{4532} promoter.

Concluding remarks

In this study, we report the presence of an internal promoter within the *sciI* T6SS gene cluster of enteroaggregative *E. coli*. The presence of internal promoters that serve as transcriptional re-starts or that are necessary to ensure proper stoichiometric production is common in large gene clusters. It has been well documented for gene clusters encoding amino-acid synthesis pathways such as histidine, tryptophan, threonine, or branched chain amino-acids (63-67). More recently, an internal promoter within the gene cluster encoding the ESX-3 type VII secretion system has been identified in *Mycobacterium smegmatis* (68). Here, we show that this internal promoter, P_{4532} , is under the control of a regulatory mechanism similar to that controlling the main promoter (Fig. 7): expression from the P_{4532} promoter is repressed by the Fur protein, that binds to a Fur box overlapping with the -10 transcriptional element. In addition, a GATC site, GATC-32, which is a target of the Dam methylase,

overlaps with the Fur binding box. In iron rich conditions, Fur binding to the promoter prevents methylation of this motif. However, during iron starvation, Fur removal allows methylation of the GATC-32 site and the methylation decreases the affinity of Fur for its binding box. Therefore Fur controls the switch between ON and OFF expression, whereas Dam methylation stabilizes the ON phase (Fig. 7). This mechanism is therefore similar to that previously reported for the *sciI* main promoter (62). However, differences can be noticed. First, the level of methylation and the activity of the Dam methylase might be slightly different on the main and the internal promoters, as the sequences flanking the GATC motifs have different AT content. Indeed, sequences flanking Dam sites have been previously shown to modulate the catalytic activity or the processivity of Dam (69). Second, a ~13-fold derepression of the internal promoter is observed in absence of Fur, while a >25-fold derepression was observed for the main promoter (62). These results are in agreement with the lower consensus of the Fur-32 box compared to the Fur box overlapping with the -10 of the main promoter (Fig. 2C), and with the potential cooperativity of the two Fur-binding boxes at the main promoter (62).

The role of the Dam methylase in transcriptional gene regulation is well documented. In addition to its role in mismatch repair and replication initiation, Dam is involved in epigenetic control of the expression of many genes including genes encoding type III secretion systems, adhesins, fimbriae, or involved in lipopolysaccharide modifications (for reviews, see 70-72). GATC sites can be found in intergenic regions, and in some cases these sites overlap with transcriptional elements such as the -10 (73). Hence Dam-dependent methylation may directly impact transcription. However, in most cases, GATC sites found in promoter regions do not overlap with transcriptional elements, but rather with regulator binding boxes. In these cases, the methylation status may control binding of the regulator, and reciprocally, regulator binding may prevent methylation of certain GATC sites. Several

studies have reported competition between Dam-dependent methylation and regulator fixation, such as the OxyR repressor at the *agn43* promoter, or the Lrp repressor at the *pap* operon promoter (74-76). In general, competition between methylation and regulator binding results in the transition between OFF and ON expression phases (72).

In conclusion, the *sciI* gene cluster is subjected to Fur/Dam regulation, and a transcriptional re-start occurs after the eighth gene of the operon. Further experiments will be necessary to define whether this re-start is necessary because transcription of the mRNA from the initial promoter stops before the last gene, or because the distal part of the operon requires additional copies of mRNA for proper stoichiometry.

MATERIAL AND METHODS

Bacterial strains, plasmids, medium, and growth conditions. *E. coli* K-12 strain DH5a was used for all cloning procedures. The EAEC strains used in this study are all derivatives of 17-2 and have been previously described (62). The plasmid-borne *P₄₅₃₂-lacZ* fusion was engineered by ligating a blunt-end 570-bp fragment encompassing the 4532 promoter (corresponding to bases -450 to +120, respective to the *EC042_4532* transcriptional start site [nucleotides 4892656-4893121], amplified from EAEC 17-2 chromosomal DNA using oligonucleotides 5'-CGCACCATGATCGTCTCTGTATCGC and 5'-CTGAAACGAACTGCTCATGGCTCTCTC) into the *Sma*I-linearized pGE573, a vector that carries a promoter-less *lacZ* gene (77). In this construct, the *lacZ* gene is under the control of the *P₄₅₃₂* promoter. Proper insertion, orientation and sequence of the fragment into the pGE-*P₄₅₃₂* plasmid were verified by restriction, PCR and DNA sequencing (MWG). *E. coli* cells were routinely grown in Luria Broth (LB) or *Sci*I-inducing medium (SIM; M9 minimal medium supplemented with glycerol 0.25 %, vitamin B1 200 µg.mL⁻¹, casaminoacids 40 µg.mL⁻¹, MgCl₂ 2 mM, CaCl₂ 0.1 mM, and LB (10% v/v); 62) supplemented with antibiotics when necessary (kanamycin 50 µg.mL⁻¹, ampicillin 100 µg.mL⁻¹ for K-12 or 200 µg.mL⁻¹ for EAEC).

RNA purification. EAEC total RNAs have been extracted using the PureYield™ RNA midiprep system (Promega) from 8×10⁹ cells grown in SIM and harvested in exponential growth phase (optical density at λ=600nm [OD₆₀₀] ~ 0.8). RNAs were eluted with 1 mL of water, cleared with DNaseI

(AmbionTM), and precipitated overnight at – 80°C by ammonium sulfate/ethanol procedures. The RNA pellet was washed and resuspended in 45 µL of nuclease-free water. RNA quality and integrity were tested on agarose gel, and by the absorbance ratio at $\lambda=260/280$ nm. The absence of DNA contamination was further tested by PCR using 35 cycles of amplification. Quantifications gave an average RNA concentration of 70 µg.mL⁻¹. Total RNAs were then subjected to RT-PCR (Access RT-PCR, Promega) or transcriptional +1 mapping (5'RACE, Invitrogen).

Reverse transcription – PCR. The Reverse transcription (RT) and PCR have been performed with the one-tube procedure, using the Access RT-PCR system (Promega), with 200 ng of total RNA and oligonucleotides allowing amplification of 550-750-bp regions overlapping the two contiguous genes (see Fig. 1A; primer sequences available upon request), following the supplier's guidelines. Briefly, both reverse transcriptase and Tfl Taq polymerase were added in each tube. The reverse transcription was carried out for 45 min at 45°C, and, after inactivation of the reverse transcriptase at 94°C for 5 min, a 30-cycle PCR was performed (denaturation at 94°C for 30 sec; annealing at 55°C for 40 sec.; and amplification at 68°C for 50 sec.). As negative controls to test for DNA contamination, RT-PCR were also performed in absence of Reverse Transcriptase. As positive controls, the regions overlapping the two contiguous genes have been amplified from 30 ng of genomic DNA.

5'-RACE assay. Total RNAs (80 µg.mL⁻¹) were subjected to transcriptional +1 mapping using the 5'RACE system (Invitrogen).

β -galactosidase assays. β -Galactosidase activity was measured by the method of Miller (78) on whole cells harvested at OD₆₀₀ of 0.8. Reported values represent the average of technical triplicates from three independent biological cultures, and standard deviation are shown on the graphs.

Protein purification. The Fur and NtrC proteins have been purified as described previously (62, 79). The σ^{70} -saturated RNAP holoenzyme has been purchased from USB Corp. The Dam methylase and restriction enzymes have been obtained from New England Biolabs and have been used as recommended by the manufacturer.

Electrophoretic Mobility gel Shift Assay (EMSA) and Dam methylation assays. DNA radiolabeling, EMSA, Fur/RNAP competition EMSA, and *in vivo* and *in vitro* Dam methylation assays have been performed as previously described (62).

Authors contribution

YRB and EC conceived the study and designed the experiments. YRB performed all in vivo and in vitro experiments, with the help of CSB for RNA analyses. YRB and EC analyzed the data. EC wrote the manuscript.

Acknowledgements

We thank Emmanuelle Bouveret and Mireille Ansaldi for sharing strains, plasmids and protocols, Laure Journet and the members of the Cascales, Llobès, Bouveret and Sturgis research groups for insightful discussions, and Isabelle Bringer, Annick Brun and Olivier Uderso for technical assistance. This work was supported by grants from the Agence Nationale de la Recherche to E.C. (ANR-10-JCJC-1303-03 and ANR-14-CE14-0006-02). Work in EC laboratory is supported by the CNRS, the Aix-Marseille Université, the Fondation pour la Recherche Médicale (DEQ20180339165), and the Fondation Bettencourt-Schueller. Y.R.B. was a recipient of a doctoral fellowship from the French Ministry of Research.

References

1. West SA, Griffin AS, Gardner A. 2007. Evolutionary explanations for cooperation. *Curr Biol* 17:661–672.
2. Blango MG, Mulvey MA. 2009. Bacterial landlines: contact-dependent signaling in bacterial populations. *Curr Opin Microbiol* 12:177–81. <https://doi.org/10.1016/j.mib.2009.01.011>.
3. Strassmann JE, Gilbert OM, Queller DC. 2011. Kin discrimination and cooperation in microbes. *Annu Rev Microbiol* 65:349–367. <https://doi.org/10.1146/annurev.micro.112408.134109>.
4. Cornforth DM, Foster KR. 2013. Competition sensing: the social side of bacterial stress responses. *Nat Rev Microbiol* 11:285–293. <https://doi.org/10.1038/nrmicro2977>.
5. Aussel L, Beuzón CR, Cascales E. 2016. Meeting report: adaptation and communication of bacterial pathogens. *Virulence* 7:481–490. <https://doi.org/10.1080/21505594.2016.1152441>.
6. Rakoff-Nahoum S, Foster KR, Comstock LE. 2016. The evolution of cooperation within the gut microbiota. *Nature* 533:255–259. <https://doi.org/10.1038/nature17626>.
7. Chassaing B, Cascales E. 2018. Antibacterial weapons: targeted destruction in the microbiota. *Trends Microbiol* 26:329–338. <https://doi.org/10.1016/j.tim.2018.01.006>.
8. García-Bayona L, Comstock LE. 2018. Bacterial antagonism in host-associated microbial communities. *Science* 361:eaat2456. <https://doi.org/10.1126/science.aat2456>.
9. Granato ET, Meiller-Legrand TA, Foster KR. 2019. The evolution and ecology of bacterial warfare. *Curr Biol* 29:521–537. <https://doi.org/10.1016/j.cub.2019.04.024>.
10. Cascales E, Buchanan SK, Duché D, Kleanthous C, Llobès R, Postle K, Riley M, Slatin S, Cavard D. 2007. Colicin biology. *Microbiol Mol Biol Rev* 71:158–229.
11. Ruhe ZC, Low DA, Hayes CS. 2013. Bacterial contact-dependent growth inhibition. *Trends Microbiol* 21:230–237. <https://doi.org/10.1016/j.tim.2013.02.003>.

12. Coulthurst S. 2019. The Type VI secretion system: a versatile bacterial weapon. *Microbiology* 165:503–515. <https://doi.org/10.1099/mic.0.000789>.
13. Ho BT, Dong TG, Mekalanos JJ. 2014. A view to a kill: the bacterial type VI secretion system. *Cell Host Microbe* 15:9–21. <https://doi.org/10.1016/j.chom.2013.11.008>.
14. Zoued A, Brunet YR, Durand E, Aschtgen MS, Logger L, Douzi B, Journet L, Cambillau C, Cascales E. 2014. Architecture and assembly of the Type VI secretion system. *Biochim Biophys Acta* 1843:1664–1673. <https://doi.org/10.1016/j.bbamcr.2014.03.018>.
15. Basler M. 2015. Type VI secretion system: secretion by a contractile nanomachine. *Philos Trans R Soc Lond B Biol Sci* 370:20150021. <https://doi.org/10.1098/rstb.2015.0021>.
16. Cascales E. 2017. Microbiology: and Amoebophilus invented the machine gun! *Curr Biol* 27:1170–1173. <https://doi.org/10.1016/j.cub.2017.09.025>.
17. Brackmann M, Nazarov S, Wang J, Basler M. 2017. Using force to punch holes: mechanics of contractile nanomachines. *Trends Cell Biol* 27:623–632. <https://doi.org/10.1016/j.tcb.2017.05.003>.
18. Taylor NMI, van Raaij MJ, Leiman PG. 2018. Contractile injection systems of bacteriophages and related systems. *Mol Microbiol* 108:6–15. <https://doi.org/10.1111/mmi.13921>.
19. Cherrak Y, Flaughnatti N, Durand E, Journet L, Cascales E. 2019. Structure and activity of the Type VI secretion system. *Microbiol Spectr* 7:0031-2019. <https://doi.org/10.1128/microbiolspec.PSIB-0031-2019>.
20. Kudryashev M, Wang RY, Brackmann M, Scherer S, Maier T, Baker D, DiMaio F, Stahlberg H, Egelman EH, Basler M. 2015. Structure of the type VI secretion system contractile sheath. *Cell* 160:952–962. <https://doi.org/10.1016/j.cell.2015.01.037>.
21. Wang J, Brackmann M, Castaño-Díez D, Kudryashev M, Goldie KN, Maier T, Stahlberg H, Basler M. 2017. Cryo-EM structure of the extended type VI secretion system sheath-tube complex. *Nat Microbiol* 2:1507–1512. <https://doi.org/10.1038/s41564-017-0020-7>.
22. Aschtgen MS, Gavioli M, Dessen A, Lloubès R, Cascales E. 2010. The SciZ protein anchors the enteroaggregative *Escherichia coli* Type VI secretion system to the cell wall. *Mol Microbiol* 75:886–899. <https://doi.org/10.1111/j.1365-2958.2009.07028.x>.
23. Zoued A, Durand E, Bebeacua C, Brunet YR, Douzi B, Cambillau C, Cascales E, Journet L. 2013. TssK is a trimeric cytoplasmic protein interacting with components of both phage-like and membrane anchoring complexes of the type VI secretion system. *J Biol Chem* 288:27031–27041. <https://doi.org/10.1074/jbc.M113.499772>.
24. English G, Byron O, Cianfanelli FR, Prescott AR, Coulthurst SJ. 2014. Biochemical analysis of TssK, a core component of the bacterial Type VI secretion system, reveals distinct oligomeric states of TssK and identifies a TssK-TssFG subcomplex. *Biochem J* 461:291–304. <https://doi.org/10.1042/BJ20131426>.
25. Brunet YR, Zoued A, Boyer F, Douzi B, Cascales E. 2015. The type VI secretion TssEFGK-VgrG phage-like baseplate is recruited to the TssJLM membrane complex via multiple contacts and serves as assembly platform for tail tube/sheath polymerization. *PLoS Genet* 11:e1005545. <https://doi.org/10.1371/journal.pgen.1005545>.
26. Durand E, Nguyen VS, Zoued A, Logger L, Péhau-Arnaudet G, Aschtgen MS, Spinelli S, Desmyter A, Bardiaux B, Dujeancourt A, Roussel A, Cambillau C, Cascales E, Fronzes R. 2015. Biogenesis and structure of a type VI secretion membrane core complex. *Nature* 523:555–560. <https://doi.org/10.1038/nature14667>.
27. Nguyen VS, Logger L, Spinelli S, Legrand P, Huyen Pham TT, Nhung Trinh TT, Cherrak Y, Zoued A, Desmyter A, Durand E, Roussel A, Kellenberger C, Cascales E, Cambillau C. 2017. Type VI secretion TssK baseplate protein exhibits structural similarity with phage receptor-binding proteins and evolved to bind the membrane complex. *Nat Microbiol* 2:17103. <https://doi.org/10.1038/nmicrobiol.2017.103>.
28. Cherrak Y, Rapisarda C, Pellarin R, Bouvier G, Bardiaux B, Allain F, Malosse C, Rey M, Chamot-Rooke J, Cascales E, Fronzes R, Durand E. 2018. Biogenesis and structure of a type VI secretion baseplate. *Nat Microbiol* 3:1404–1416. <https://doi.org/10.1038/s41564-018-0260-1>.
29. Rapisarda C, Cherrak Y, Kooger R, Schmidt V, Pellarin R, Logger L, Cascales E, Pilhofer M, Durand E, Fronzes R. 2019. In situ and high-resolution cryo-EM structure of a bacterial type VI

- secretion system membrane complex. *EMBO J* 38:e100886. <https://doi.org/10.15252/embj.2018100886>.
30. Basler M, Pilhofer M, Henderson GP, Jensen GJ, Mekalanos JJ. 2012. Type VI secretion requires a dynamic contractile phage tail-like structure. *Nature* 483:182–186. <https://doi.org/10.1038/nature10846>.
 31. Brunet YR, Espinosa L, Harchouni S, Mignot T, Cascales E. 2013. Imaging type VI secretion-mediated bacterial killing. *Cell Rep* 3:36–41. <https://doi.org/10.1016/j.celrep.2012.11.027>.
 32. Kapitein N, Bönemann G, Pietrosiuk A, Seyffer F, Hausser I, Locker JK, Mogk A. 2013. ClpV recycles VipA/VipB tubules and prevents non-productive tubule formation to ensure efficient type VI protein secretion. *Mol Microbiol* 87:1013–1028. <https://doi.org/10.1111/mmi.12147>.
 33. Cascales E, Cambillau C. 2012. Structural biology of type VI secretion systems. *Philos Trans R Soc Lond B Biol Sci* 367:1102–1111. <https://doi.org/10.1098/rstb.2011.0209>.
 34. LeRoux M, De Leon JA, Kuwada NJ, Russell AB, Pinto-Santini D, Hood RD, Agnello DM, Robertson SM, Wiggins PA, Mougous JD. 2012. Quantitative single-cell characterization of bacterial interactions reveals type VI secretion is a double-edged sword. *Proc Natl Acad Sci USA* 109:19804–19809. <https://doi.org/10.1073/pnas.1213963109>.
 35. Basler M, Ho BT, Mekalanos JJ. 2013. Tit-for-tat: type VI secretion system counterattack during bacterial cell-cell interactions. *Cell* 152:884–894. <https://doi.org/10.1016/j.cell.2013.01.042>.
 36. Silverman JM, Agnello DM, Zheng H, Andrews BT, Li M, Catalano CE, Gonen T, Mougous JD. 2013. Haemolysin coregulated protein is an exported receptor and chaperone of type VI secretion substrates. *Mol Cell* 51:584–593. <https://doi.org/10.1016/j.molcel.2013.07.025>.
 37. Shneider MM, Buth SA, Ho BT, Basler M, Mekalanos JJ, Leiman PG. 2013. PAAR-repeat proteins sharpen and diversify the type VI secretion system spike. *Nature* 500:350–353. <https://doi.org/10.1038/nature12453>.
 38. Durand E, Cambillau C, Cascales E, Journet L. 2014. VgrG, Tae, Tle, and beyond: the versatile arsenal of Type VI secretion effectors. *Trends Microbiol* 22:498–507. <https://doi.org/10.1016/j.tim.2014.06.004>.
 39. Whitney JC, Beck CM, Goo YA, Russell AB, Harding BN, De Leon JA, Cunningham DA, Tran BQ, Low DA, Goodlett DR, Hayes CS, Mougous JD. 2014. Genetically distinct pathways guide effector export through the type VI secretion system. *Mol Microbiol* 92:529–542. <https://doi.org/10.1111/mmi.12571>.
 40. Alcoforado Diniz J, Coulthurst SJ. 2015. Intraspecies competition in *Serratia marcescens* is mediated by Type VI-secreted Rhs effectors and a conserved effector-associated accessory protein. *J Bacteriol* 197:2350–2360. <https://doi.org/10.1128/JB.00199-15>.
 41. Alcoforado Diniz J, Liu YC, Coulthurst SJ. 2015. Molecular weaponry: diverse effectors delivered by the Type VI secretion system. *Cell Microbiol* 17:1742–1751. <https://doi.org/10.1111/cmi.12532>.
 42. Unterweger D, Kostiuk B, Ötjengerdes R, Wilton A, Diaz-Satizabal L, Pukatzki S. 2015. Chimeric adaptor proteins translocate diverse type VI secretion system effectors in *Vibrio cholerae*. *EMBO J* 34:2198–2210. <https://doi.org/10.15252/embj.201591163>.
 43. Whitney JC, Quentin D, Sawai S, LeRoux M, Harding BN, Ledvina HE, Tran BQ, Robinson H, Goo YA, Goodlett DR, Raunser S, Mougous JD. 2015. An interbacterial NAD(P)(+) glycohydrolase toxin requires elongation factor Tu for delivery to target cells. *Cell* 163:607–619. <https://doi.org/10.1016/j.cell.2015.09.027>.
 44. Flaugnatti N, Le TT, Canaan S, Aschtgen MS, Nguyen VS, Blangy S, Kellenberger C, Roussel A, Cambillau C, Cascales E, Journet L. 2015. A phospholipase A(1) antibacterial Type VI secretion effector interacts directly with the C-terminal domain of the VgrG spike protein for delivery. *Mol Microbiol* 99:1099–1118. <https://doi.org/10.1111/mmi.13292>.
 45. Unterweger D, Kostiuk B, Pukatzki S. 2017. Adaptor proteins of Type VI secretion system effectors. *Trends Microbiol* 25:8–10. <https://doi.org/10.1016/j.tim.2016.10.003>.
 46. Coyne MJ, Comstock LE. 2019. Type VI secretion systems and the gut microbiota. *Microbiol Spectr* 7:0009-2018. <https://doi.org/10.1128/microbiolspec.PSIB-0009-2018>.

47. Fu Y, Waldor MK, Mekalanos JJ. 2013. Tn-Seq analysis of *Vibrio cholerae* intestinal colonization reveals a role for T6SS-mediated antibacterial activity in the host. *Cell Host Microbe* 14:652–663. <https://doi.org/10.1016/j.chom.2013.11.001>.
48. Bachmann V, Kostiuik B, Unterweger D, Diaz-Satizabal L, Ogg S, Pukatzki S. 2015. Bile salts modulate the mucin-activated Type VI secretion system of pandemic *Vibrio cholerae*. *PLoS Negl Trop Dis* 9:e0004031. <https://doi.org/10.1371/journal.pntd.0004031>.
49. Wexler AG, Bao Y, Whitney JC, Bobay LM, Xavier JB, Schofield WB, Barry NA, Russell AB, Tran BQ, Goo YA, Goodlett DR, Ochman H, Mougous JD, Goodman AL. 2016. Human symbionts inject and neutralize antibacterial toxins to persist in the gut. *Proc Natl Acad Sci USA* 113:3639–3644. <https://doi.org/10.1073/pnas.1525637113>.
50. Sana TG, Flaughnatti N, Lugo KA, Lam LH, Jacobson A, Baylot V, Durand E, Journet L, Cascales E, Monack DM. 2016. *Salmonella Typhimurium* utilizes a T6SS-mediated antibacterial weapon to establish in the host gut. *Proc Natl Acad Sci USA* 113:5044–5051. <https://doi.org/10.1073/pnas.1608858113>.
51. Anderson MC, Vonaesch P, Saffarian A, Marteyn BS, Sansonetti PJ. 2017. *Shigella sonnei* encodes a functional T6SS used for interbacterial competition and niche occupancy. *Cell Host Microbe* 21:769–776. <https://doi.org/10.1016/j.chom.2017.05.004>.
52. Bernard CS, Brunet YR, Gueguen E, Cascales E. 2010. Nooks and crannies in type VI secretion regulation. *J Bacteriol* 192:3850–3860. <https://doi.org/10.1128/JB.00370-10>.
53. Leung KY, Siame BA, Snowball H, Mok YK. 2011. Type VI secretion regulation: crosstalk and intracellular communication. *Curr Opin Microbiol* 14:9–15. <https://doi.org/10.1016/j.mib.2010.09.017>.
54. Silverman JM, Brunet YR, Cascales E, Mougous JD. 2012. Structure and regulation of the type VI secretion system. *Annu Rev Microbiol* 66:453–472. <https://doi.org/10.1146/annurev-micro-121809-151619>.
55. Miyata ST, Bachmann V, Pukatzki S. 2013. Type VI secretion system regulation as a consequence of evolutionary pressure. *J Med Microbiol* 62:663–676. <https://doi.org/10.1099/jmm.0.053983-0>.
56. LeRoux M, Kirkpatrick RL, Montauti EI, Tran BQ, Peterson SB, Harding BN, Whitney JC, Russell AB, Traxler B, Goo YA, Goodlett DR, Wiggins PA, Mougous JD. 2015. Kin cell lysis is a danger signal that activates antibacterial pathways of *Pseudomonas aeruginosa*. *Elife* 4. <https://doi.org/10.7554/eLife.05701>.
57. LeRoux M, Peterson SB, Mougous JD. 2015. Bacterial danger sensing. *J Mol Biol* 427:3744–3753. <https://doi.org/10.1016/j.jmb.2015.09.018>.
58. Mougous JD, Gifford CA, Ramsdell TL, Mekalanos JJ. 2007. Threonine phosphorylation post-translationally regulates protein secretion in *Pseudomonas aeruginosa*. *Nat Cell Biol* 9:797–803.
59. Dudley EG, Thomson NR, Parkhill J, Morin NP, Nataro JP. 2006. Proteomic and microarray characterization of the AggR regulon identifies a pheU pathogenicity island in enteroaggregative *Escherichia coli*. *Mol Microbiol* 61:1267–1282.
60. Journet L, Cascales E. 2016. The Type VI secretion system in *Escherichia coli* and related species. *EcoSalPlus* 7:1–20. <https://doi.org/10.1128/ecosalplus.ESP-0009-2015>.
61. Morin N, Santiago AE, Ernst RK, Guillot SJ, Nataro JP. 2013. Characterization of the AggR regulon in enteroaggregative *Escherichia coli*. *Infect Immun* 81:122–132. <https://doi.org/10.1128/IAI.00676-12>.
62. Brunet YR, Bernard CS, Gavioli M, Lloubès R, Cascales E. 2011. An epigenetic switch involving overlapping fur and DNA methylation optimizes expression of a type VI secretion gene cluster. *PLoS Genet* 7:e1002205. <https://doi.org/10.1371/journal.pgen.1002205>.
63. Grisolia V, Carlomagno MS, Bruni CB. 1982. Cloning and expression of the distal portion of the histidine operon of *Escherichia coli* K-12. *J Bacteriol* 151:692–700.
64. Grisolia V, Riccio A, Bruni CB. 1983. Structure and function of the internal promoter (hisBp) of the *Escherichia coli* K-12 histidine operon. *J Bacteriol* 155:1288–1296.
65. Jackson EN, Yanofsky C. 1972. Internal promoter of the tryptophan operon of *Escherichia coli* is located in a structural gene. *J Mol Biol* 69:307–313.

66. Saint Girons I, Margarita D. 1985. Evidence for an internal promoter in the *Escherichia coli* threonine operon. *J Bacteriol* 161:461–462.
67. Wek RC, Hatfield GW. 1986. Examination of the internal promoter, PE, in the *ilvGMEDA* operon of *E. coli* K-12. *Nucleic Acids Res* 14:2763–2777.
68. Maciag A, Piazza A, Riccardi G, Milano A. 2009. Transcriptional analysis of ESAT-6 cluster 3 in *Mycobacterium smegmatis*. *BMC Microbiol* 9:48. [https://doi: 10.1186/1471-2180-9-48](https://doi.org/10.1186/1471-2180-9-48).
69. Peterson SN, Reich NO. 2006. GATC flanking sequences regulate Dam activity: evidence for how Dam specificity may influence pap expression. *J Mol Biol* 355:459–472.
70. Wion D, Casadesús J. 2006. N6-methyl-adenine: an epigenetic signal for DNA-protein interactions. *Nat Rev Microbiol* 4:183–192.
71. Casadesús J, Low D. 2006. Epigenetic gene regulation in the bacterial world. *Microbiol Mol Biol Rev* 70:830–86.
72. Sánchez-Romero MA, Casadesús J. 2020. The bacterial epigenome. *Nat Rev Microbiol* 18:7–20. [https://doi: 10.1038/s41579-019-0286-2](https://doi.org/10.1038/s41579-019-0286-2).
73. Camacho EM, Serna A, Madrid C, Marqués S, Fernández R, de la Cruz F, Juárez A, Casadesús J. 2005. Regulation of *finP* transcription by DNA adenine methylation in the virulence plasmid of *Salmonella enterica*. *J Bacteriol* 187:5691–5699.
74. Haagmans W, van der Woude M. 2000. Phase variation of Ag43 in *Escherichia coli*: Dam-dependent methylation abrogates OxyR binding and OxyR-mediated repression of transcription. *Mol Microbiol* 35:877–887.
75. Waldron DE, Owen P, Dorman CJ. 2002. Competitive interaction of the OxyR DNA-binding protein and the Dam methylase at the antigen 43 gene regulatory region in *Escherichia coli*. *Mol Microbiol* 44:509–520.
76. Peterson SN, Reich NO. 2008. Competitive Lrp and Dam assembly at the pap regulatory region: implications for mechanisms of epigenetic regulation. *J Mol Biol* 383:92–105. [https://doi: 10.1016/j.jmb.2008.07.086](https://doi.org/10.1016/j.jmb.2008.07.086).
77. Eraso JM, Weinstock GM. 1992. Anaerobic control of colicin E1 production. *J Bacteriol* 174:5101–5109.
78. Miller, J. 1972. Experiments in Molecular Genetics, p. 352-355. Cold Spring Harbor Laboratory, NY.
79. Bernard CS, Brunet YR, Gavioli M, Lloubès R, Cascales E. 2011. Regulation of type VI secretion gene clusters by sigma54 and cognate enhancer binding proteins. *J Bacteriol* 193:2158–2167. <https://doi.org/10.1128/JB.00029-11>.

LEGEND TO FIGURES

FIG 1 Operon structure of the EAEC *sciI* T6SS gene cluster. (A) Schematic organization of the EAEC *sciI* T6SS gene cluster (*EC042_4524* to *EC042_4545*). Genes encoding T6SS core components are indicated in grey. Accessory genes or of unknown function are represented in white. The fragments corresponding to gene junctions and amplified in the RT-PCR experiments are indicated below (1, 692-bp; 2, 672-bp; 3, 550-bp; 4, 618-bp; 5, 586-bp; 6, 643-bp; 7, 748-bp; 8, 629-bp; 9, 575-bp; 10, 654-bp; 11, 581-bp; 12, 768-bp; 13, 762-bp; 14, 459-bp; 15, 600-bp; 16, 673-bp; 17, 576-bp; 18, 720-bp; 19, 552-bp; 20, 591-bp; 21, 678-bp). (B) Operon structure of the EAEC *sciI* T6SS gene cluster. Agarose gel analyses of the indicated gene junctions (numbered 1-22, see panel A) amplified by PCR from cDNA (upper panel), genomic DNA (middle panel; positive control) and total RNA (lower panel, negative control). The presence of PCR fragment in the cDNA gels demonstrates co-

transcription of the genes located in 5' and 3' of the amplified region. Molecular weight markers (MW, in kb) are indicated on the left. White dashed lines separate different gels combined to a single image.

FIG 2 Regulatory elements of the *sci1* and *4532* promoters. Nucleotide sequences of the *sci1* (A) and *EC042_4532* (B) promoters highlighting overlaps between the transcriptional elements, Fur binding boxes and Dam methylation motifs. The +1 transcriptional site, identified by 5'-RACE are indicated in bold red letters. GATC Dam methylation sites are indicated in bold blue letters. The -10 elements are indicated in green. The underlined sequences indicate Fur binding boxes (italics) and translational start codons. (C) Sequence alignment of the *fur1* (*sci1* promoter) and *fur-32* (*EC042_4532* promoter) boxes with the *E. coli* Fur box consensus sequence. Identical bases are framed in grey. The -10 elements (green letters) and GATC motifs (bold blue letters) are indicated.

FIG 3 The *4532* promoter is under the control of iron levels, Fur and Dam. β -galactosidase activity (in Miller units) of a promoterless *lacZ* fusion (white bars) and of the *P₄₅₃₂-lacZ* reporter fusion (blue bars) at OD₆₀₀=0.8 in the WT EAEC 17-2 strain, after a 30-min treatment with 2,2'-dipyridyl (+dip; 100 μ M) or in the isogenic *fur*, *dam* and *fur-dam* mutants.

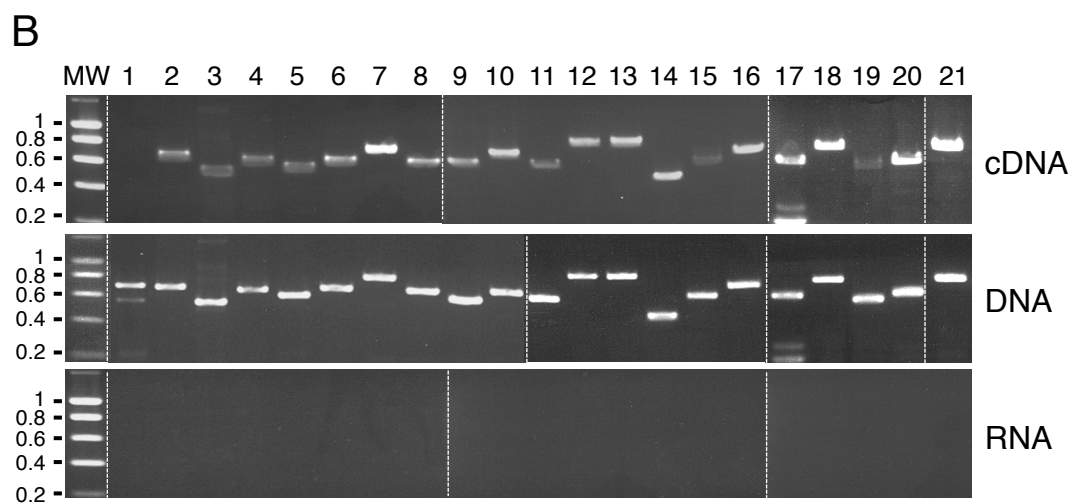
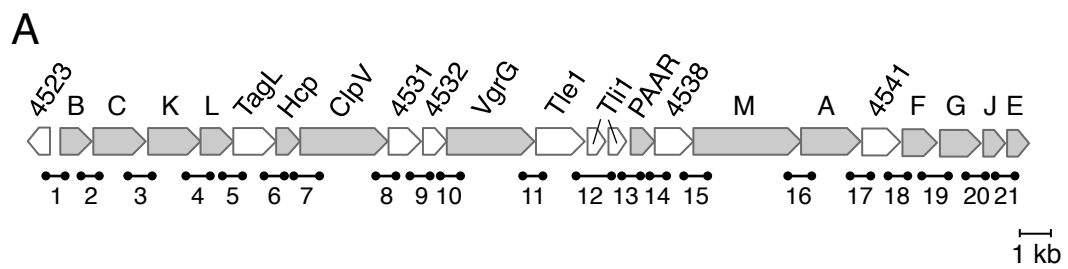
FIG 4 Fur binds to the *4532* promoter and prevents access to the RNA polymerase *in vitro*. (A) Electrophoretic mobility shift assay of the *EC042_4532* promoter (*P₄₅₃₂*) with the indicated concentration of Fur in presence of FeCl₃ or in presence of EDTA (lane 6) or using purified NtrC transcriptional activator (lane 7). Controls include Fur shift assays of the Fur-dependent *sci1* promoter (lanes 8 and 9) or of the Fur-independent *sci2* promoter (lane 10). DNA-Fur complexes are indicated by stars. The densitometry analysis of Fur binding on the *P₄₅₃₂* fragment (represented as free *P₄₅₃₂* DNA as a function of Fur concentration) is shown in panel (B). (C) Electrophoretic mobility shift assay of the unmethylated (*P₄₅₃₂*, lanes 1-6) or methylated (me-*P₄₅₃₂*, lanes 7-9) *EC042_4532* promoter with the indicated concentration of σ^{70} -RNAP (in units) alone (lanes 1-3) or in presence of 20 nM of Fur (lanes 4-6). DNA-Fur and DNA-RNAP complexes are indicated by the star and circle respectively. The densitometry analysis of RNAP binding on the unmethylated (blue curve), methylated (green curve) or Fur-bound unmethylated (red curve) *P₄₅₃₂* fragment (represented as RNAP-bound DNA as a function of RNAP concentration) is shown in panel (D).

FIG 5 Fur protects GATC-32 from methylation *in vitro* and *in vivo*. (A) A radiolabeled PCR product corresponding to the 570-bp *P₄₅₃₂* fragment was digested by the restriction enzymes indicated on top. Left panel, untreated PCR product; middle panel, PCR product treated with the Dam methylase; right panel, PCR product incubated with purified Fur (20 nM) prior to Dam methylation. Molecular weight markers (MW, in bp) are indicated on the left. The sizes of the digestion products (in bp) are indicated on the right. See Suppl. Fig. S2 for positions of restriction sites and sizes of expected DNA fragments. (B) The *P₄₅₃₂* promoters isolated from pGE573 vectors carrying the *P₄₅₃₂-lacZ* fusion purified from the

EAEC wild-type strain (WT, left panel) or its isogenic *dam* (second panel from left) or *fur* (right panel) mutant strains, or from the WT strain treated with 2,2'-dipyridyl (third panel from left) were digested by the restriction enzymes indicated on top. Molecular weight markers (MW, in bp) are indicated on the left. The sizes of the digestion products (in bp) are indicated on the right. The white dashed lines in left panel indicate reorganization of the lines from the same gel. See Suppl. Fig. S2 for positions of restriction sites and sizes of expected DNA fragments.

FIG 6 GATC-32 methylation influences Fur binding on P_{4532} . (A) Electrophoretic mobility shift assay of the unmethylated (P_{4532}) or methylated (me- P_{4532}) P_{4532} fragment with the indicated concentration of purified Fur. The densitometry analysis of Fur binding on the unmethylated (blue curve) or methylated (green curve) P_{4532} fragment (represented as free P_{4532} DNA as a function of Fur concentration) is shown in panel (B).

FIG 7 Schematic representation of *sciI* gene cluster regulation. (A) The *sciI* T6SS gene cluster is represented on top with the location of the main (P_{SciI}) and internal (P_{4532}) promoters. Zoom-in genetic architectures of these promoters are shown at bottom (+1, transcriptional start; -10 and -35 transcriptional elements [blue]; Fur binding box [orange]; Dam methylation GATC site [green]). (B) Model of regulation of *sciI* main and internal promoters by Fur and Dam. In iron-replete conditions (left), a Fur dimer (orange hexagons) complexed to iron (black dots) is bound to the Fur box, preventing methylation of the GATC site, and access to the RNA polymerase. Expression from the promoter is repressed (OFF state). In iron-limiting conditions (right), Fur is released from the promoter, allowing GATC methylation by Dam and binding of the RNA polymerase. Expression from the promoter is turned on (ON state).



A *P_{sci1}*

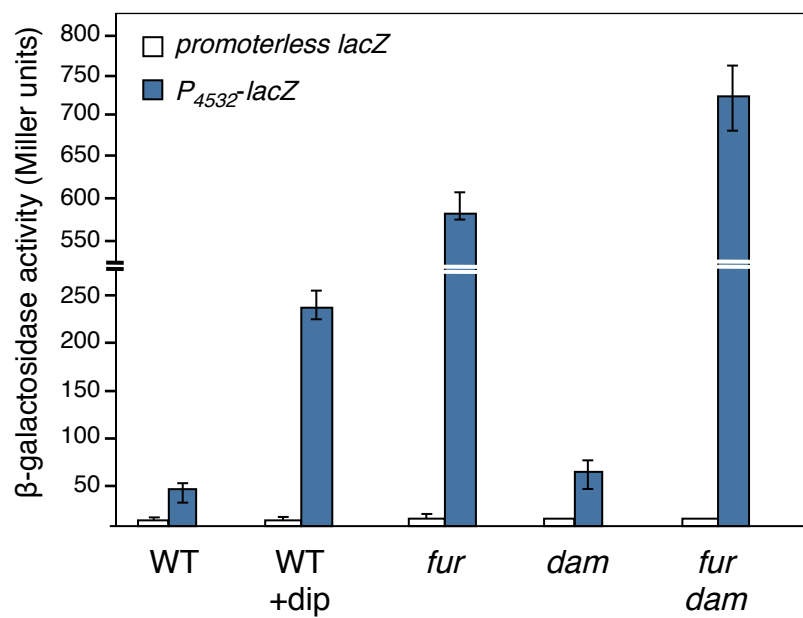
CCTGATTATTTGCATTATATC**GATC**GATGTATCTG
TTATATTGAGATTTTTTC**GATC**TTCGTCCTATAAT
GATCAAAATTAAATCAGTGCACAAGGGGAGGCATC
TGCGGTGATGGAACCCCTGAGATGCAGGTTTCACA
GGAGAGAGCCATG

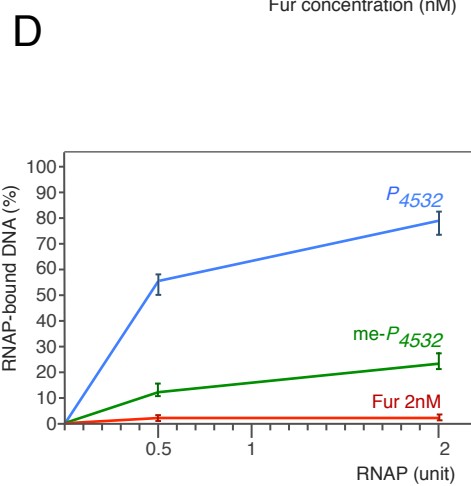
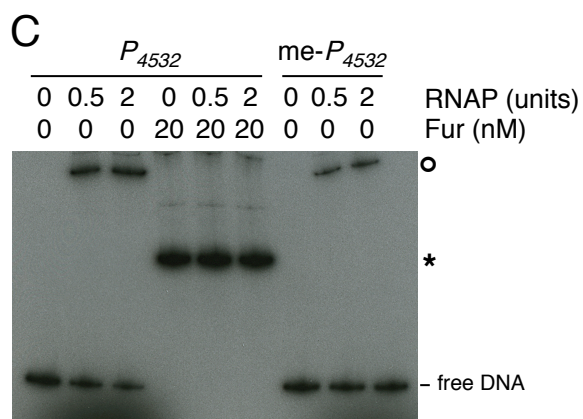
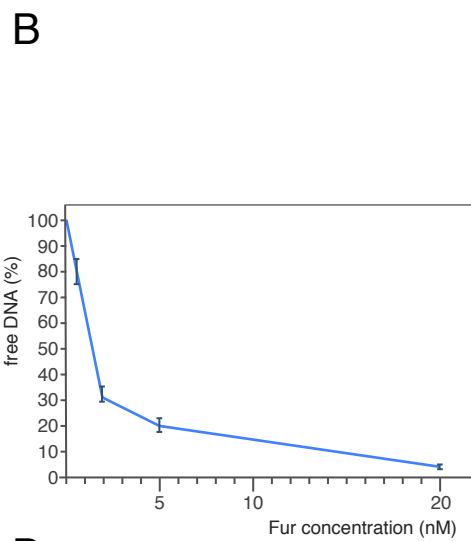
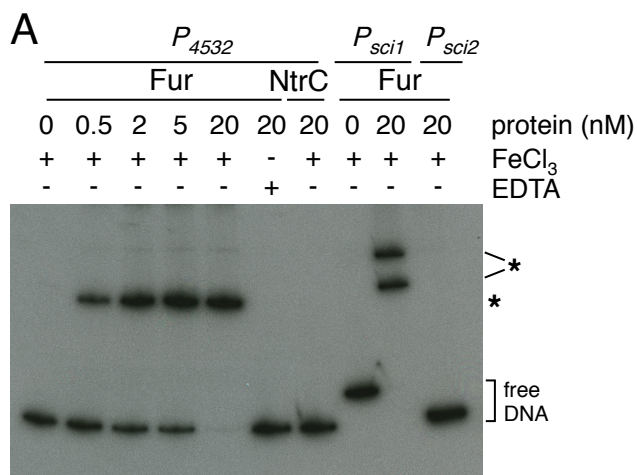
B *P₄₅₃₂*

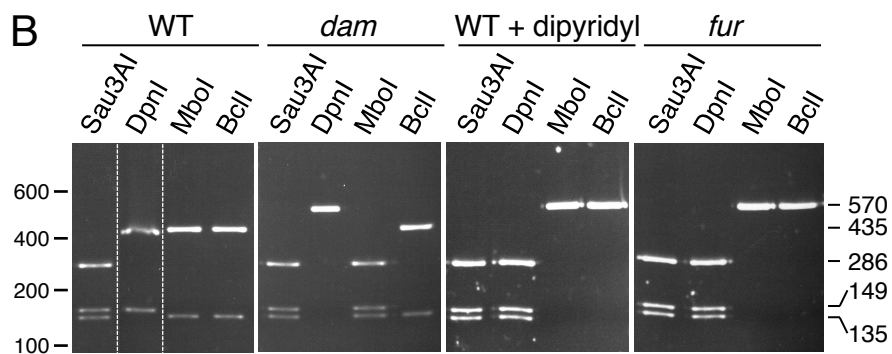
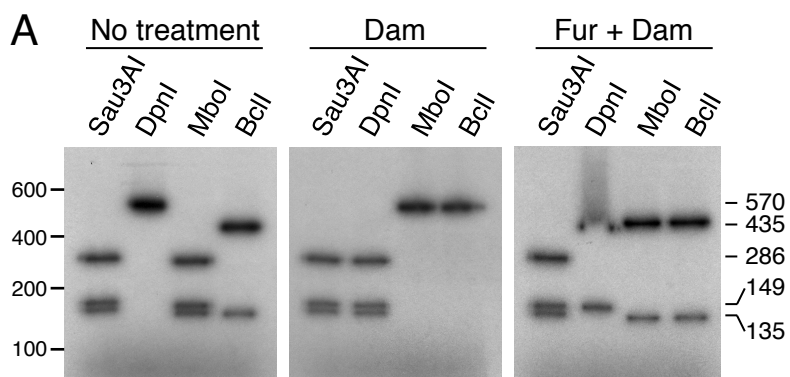
GCGAATATCCCATGGAGCAGCAGGCACAAATTATT
GCT**GATC**ATTTTACTTTGCA**G**GCTGAAGGATACGG
GACATGGTGTGATATGAGAAGGGACGGTGATATCA
CACTGGACGGAAATATGTCTGAGTATGTTATTCGC
AGCCTGTATACCAGCACGTTGCGGGGGTTCCCATG

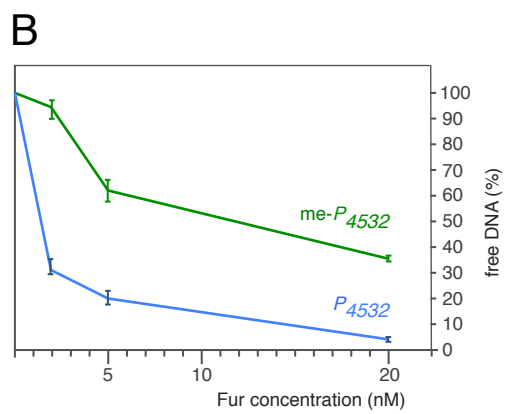
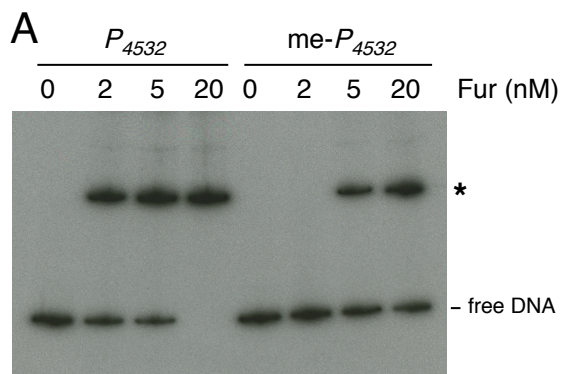
C

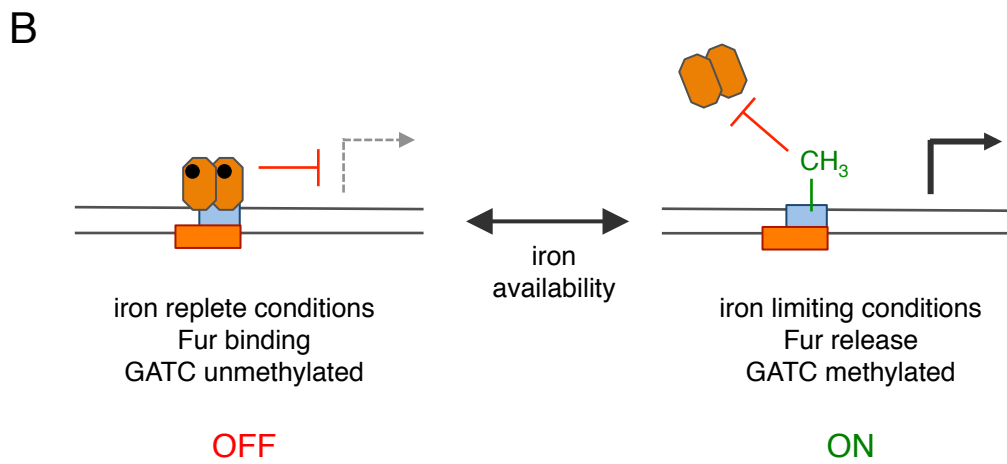
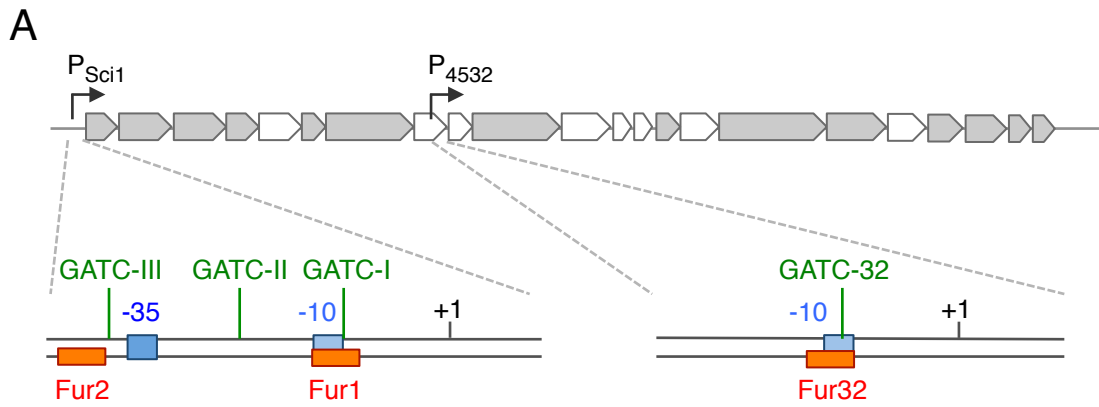
Fur1	TATAAT GATC AAAATTAAA
Fur box	GATAATGATAATCATTATC
Fur-32	ATTATTGCT GATC ATTTTA



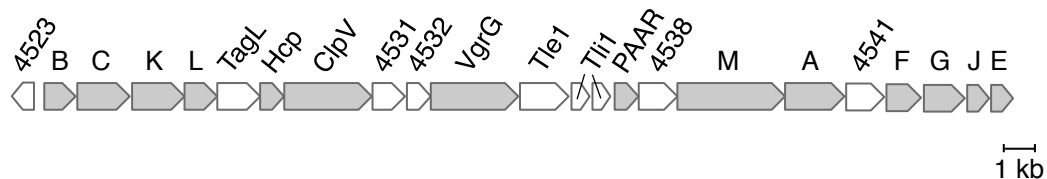








A



B

<i>tssB-tssC</i> TGA(N) ₂₁ atg	<i>tssC-tssK</i> TAA(N) ₁₅ atg	<i>tssK-tssL</i> <u>caTGA</u> at -4	<i>tssL-tagL</i> TAA(N) ₂ atg
<i>tagL-hcp</i> TAA(N) ₅ atg	<i>hcp-clpV</i> TAA(N) ₁₅₉ gtg	<i>clpV-4531</i> <u>ttaTGA</u> acc -4	<i>4531-4532</i> <u>atggTAA</u> -7
<i>4532-vgrG</i> <u>atgaatctcacTGA</u> -14	<i>vgrG-tle1</i> gaa TGA ca -4	<i>tle1-tli1</i> TAA(N) ₁₉ atg	<i>tli1b-PAAR</i> TGA(N) ₃₁ atg
<i>PAAR-4538</i> TAA(N) ₃ atg	<i>4538-tssM</i> aa <u>atg</u> aaTAAa -8	<i>tssM-tssA</i> gacTG A tggt -1	<i>tssA-4541</i> TGAgat g
<i>4541-tssF</i> TGA(N) ₇ atg	<i>tssF-tssG</i> <u>atg(N)₄₀TAA</u> -46	<i>tssG-tssJ</i> <u>atg(N)₁₄TAA</u> -20	<i>tssJ-tssE</i> TAG(N) ₂ atg

